RESEARCH ARTICLE OPEN ACCESS

Plasma Nitriding Effect on Tribological Behavior of AISI D2 tool steel: Understanding of Wear Rate

Marcos Dorigão Manfrinato[1,2], Fernando Falchi Fiaschi[3], Miguel Rubira Danelon[2], Larissa Solano de Almeida[2], Ronaldo Câmara Cozza[4,5], Luciana Sgarbi Rossino[1,2]

Sorocaba Technological College (FATEC Sorocaba), Sorocaba, SP, Brazil
Email: marcos.manfrinato@fatec.sp.gov.br
[2] Federal University of São Carlos – UFSCar Campus Sorocaba, Pos-Graduate Program in Materials Science (PPGCM), Sorocaba, SP, Brazil
Navy Technological Center in São Paulo (ARAMAR), Iperó, SP, Brazil
Mauá Technological College (FATEC Mauá), Mauá, SP, Brazil
[5] Department of Mechanical Engineering, University Center FEI – Educational Foundation of Ignatius "Priest Sabóia de Medeiros", São Bernardo do Campo, SP, Brazil

ABSTRACT
Plasma nitriding increases tool steels life. In the Steady-State of wear (SSW) the wear coefficient (k - wear rate) as a function of the sliding distance and applied load does not change and allows the development of mathematical models to predict the wear behavior of the material under the test conditions. The AISI D2 steel was plasma nitrided at 480°C (80%N2/20%H2) for 4h. The nitrided layer has a thickness of 80μm and a composite layer of 2.46μm. The increase in hardness in the nitrided sample improved the wear resistance of the material studied. In addition, it was possible to obtain the SSW of the material and determine the constant k through mathematical models that allow the prediction of wear behavior. Thus, plasma nitriding treatment was effective to improve the wear resistance of AISI D2, and SSW is an important parameter to predict the wear behavior of materials.

Keywords – microwear, AISI D2, nitriding, wear rate

Date of Submission: 10-11-2022 Date of Acceptance: 23-11-2022

I. INTRODUCTION

AISI D2 is a cold working tool steel, which has the properties of high hardenability, high softening resistance, and wear resistance, among other properties, due to its high carbon and chromium content in the alloy. Because of those properties, this steel is applied to the cold forming of different materials in the industry. Such applications compromise the tool useful life, due to the high stress applied in service, encouraging surface modification studies of AISI D2 steels through surface treatments, which promote a longer useful life of the tool [1] [2].

Thermochemical treatments assisted by plasma are attractive to steel application, as plasma nitriding, which improves the wear, fatigue, and corrosion resistance of the material, due to a surface modification caused by nitrogen diffusion and combination with other elements present in the material, forming a compound layer and diffusion zone, regions that present high hardness when compared to the substrate [3], [4], [5], [6].

In the nitriding treatment, two different kinds of nitrides are commonly found, the Fe_4N nitride, called γ' phase with the crystalline structure of FCC (Face Centered Cubic), which promotes ductility to the layer, and $Fe_{2-3}N$, called ε phase, presenting CH structure (Compact Hexagonal) corresponding to a nitride with higher hardness and consequently more fragile when compared to the other nitride type cited previously [7], [8], [9]. In addition to the compound layer, the formation of the diffusion zone also occurs, which consists of a supersaturated interstitial solid solution of nitrogen in iron, whose layer is formed by the nitrogen released during the decomposition process of unstable nitrides [7].

The surface hardness of a material influences its wear resistance, improving the tribological behavior and reducing the wear rate of the material. However, as studied by Danelon et al [8], the hardness is not the main parameter that

influences the wear resistance of the material, so other parameters such as thickness, uniformity of the layer, and different types of nitride can also improve or impair the wear performance of the material [8], [10].

The wear behavior in metallic materials can be evaluated by the micro-abrasive wear test by fixed ball, which has the purpose of generating a worn region with an impression in sphere shape produced on the sample by the contact of a ball with the metal surfaces [11],[12]. Knowing the crater diameter, the wear volume (V) can be determined [13],[14].

Another important piece of information to evaluate the tribological behavior of the materials, that can be obtained by the micro-abrasive wear test is the determination of the SSW, which occurs when the wear coefficient (k) tends to keep constant at the function of time or sliding distance. The tribological behavior of the tested material cannot be estimated before reaching the SSW during the test, only after this, the development of the wear process of the material can be analyzed [15].

The constancy of wear coefficient (k) represents the SSW when it presents a linear relation in the function of test time or sliding distance. This linear variation, along with a mathematical model allows the predicting of wear behavior in conditions that have not been tested in the same sample, so that can be applied to predict the wear behavior of tools during service [15],[16].

The objective of this work is to evaluate the influence of plasma nitriding treatment on wear resistance of AISI D2 steel through micro-abrasive wear test by fixed ball, understand the SSW for the treated and untreated material, and the development of the mathematical model for previsions of tribological behaviors in different test conditions.

II. MATERIALS AND METHODS

AISI D2 tool steel samples with dimensions of 25x20x15 mm were used in the development of this work, whose chemical composition is presented in Table 1, determined by the spectrometer Ametek Spectromaxx model LMF05, according to ASTM A681 standard.

Table 1 – Chemical composition of AISI D2 tool steel (wt%)

AISI D2	Nominal	Obtained
C	1.4 – 1.6	1.43
Mn	0.1 – 0.6	0.45
Si	0.1 – 0.6	0.43
Cr	11 - 13	12.1
V	0.5 – 1.1	0.81
Mo	0.7 – 1.2	0.96
P	0.03	0.015
S	0.03	0.024

Plasma nitriding was carried out in the LabTES (Surface Treatment and Engineering Laboratory) located at the Sorocaba Technological College – FATEC Sorocaba. The treatment system consists of a cylindric stainless steel hermetically closed, and a vacuum chamber generated by a mechanical rotary vane vacuum pump. Plasma was generated by a pulsed-DC power supply with a digital control system. The treatment gases were inserted into the chamber from individual cylinders through digital flowmeters. For the pressure measurement in the reactor chamber, it was utilized a Pirani gauge and the treatment temperature was controlled by a multimeter connected in a thermocouple type K, coupled to a sample positioned at the reactor cathode, as described by Cruz et. al. [17].

Before being placed in the reactor chamber for the treatment, the samples were ground, polished, cleaned with detergent and alcohol in ultrasonic cleaning, and dried. After being placed in the reactor, the system was evacuated to low vacuum pressure. The treatment began with the plasma ablation process to clean and removed the surface oxides [18]. Immediately after this step, the nitriding was performed, whose parameters are presented in Table 2.

Table 2 – Treatment parameters of plasma ablation and nitriding step.

Treatment	Gas Mixture (%)	T(ºC)	Pressure (torr)	Time (h)
Ablation (Cleaning)	80Ar-20H_2	485	2.0	1
Nitriding	80N_2 – 20H_2		3.5	4

2.1 Metallographic Analysis

The metallographic analyses were performed following the ASTM E395-00 standard. The samples were cut across the nitride samples surface, embedded with bakelite, ground in water sandpaper with a granulometry of 220, 320, 400, 600, and 1200, polished using a diamond paste of 3μm and chemically attacked using Nital 3% (97% Ethyl Alcohol – 3% Nitric Acid). The micrographic analysis was carried out by optical microscopy (OM) using a Carl Zeiss microscope model Axio Imager M2M with an acquisition image camera of 10 megapixels and Axiovision capture software. The micrographic analysis by Scanning Electron Microscopy (SEM) was carried out using Carl Zeiss

equipment, model Evo MA15, and the software Smart SEM. It was also utilized an Energy Dispersion Spectrometer (EDS) by Bruker model Quantax with the software Sprti 2.1 coupled to SEM to identify the semi-quantitative chemical elements present in the sample.

2.2 Microhardness Test

Vickers microhardness tests were performed according to the ASTM E348-99 standard with a 0.2 kgf load and application time of 15s in a Mitutoyo microdurometer, HM-200 series with a Vickers indenter. The hardness profile was determined by the hardness measures in-depth in three different positions.

2.3 Micro-Abrasive Wear Test

The micro-abrasive wear tests by fixed ball were carried out to determine the wear resistance and the friction coefficient of the treated and untreated materials. The equipment (Figure 1), located in LabTES, was equipped with two load cells to measure the normal and tangential load and determine the friction coefficient. A test ball of AISI 52100 steel was used with a hardness of 60 HRC and a diameter of 25,4mm. The test parameters used in the tests were a rotation frequency of 200 RPM, a normal load of 20N, and the test time was varied in 120, 300, 450, 600, 750, 900, 1050, and 1200 seconds. The wear volume (V) and wear coefficient (k) were calculated by eq. (1) and eq. (2) respectively, where b is the crater diameter, R is the ball radius, S is the sliding distance and N is the normal load. The measurement of the craters formed during the wear test was determined by a stereoscope with 500x magnification and analysis software.

$$V = \frac{\pi . b^4}{64 . R} \qquad \text{(eq. 1)}$$

$$K = \frac{1}{S . N} . \frac{\pi . b^4}{64 . R} \qquad \text{(eq. 2)}$$

Figure 1 – Schematic view of the micro-abrasive wear teste by fixed ball equipment

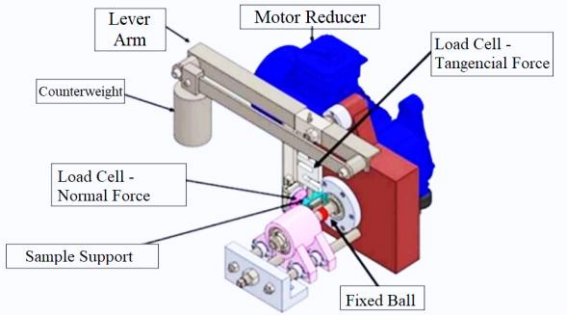

Adapted from DANELON et al., 2020.

III. RESULTS AND DISCUSSION

3.1 – Metallographic Analysis

The metallographic and EDS analysis of the treated material are presented in Figure 2. Figure 2(a) shows a total nitrided layer with a thickness of 80 µm. Precipitates observed in the diffusion zone and on the substrate are from the AISI D2 alloy elements. In Figure 2(c), it is possible to observe the compound layer, indicated by the yellow arrow, with a thickness of 2.46µm.

Figure 2 – Micrography of AISI D2 nitrided obtained by a) OM at 50x b) EDS analysis by SEM of precipitate and diffusion zone c) SEM at 5000x and EDS analysis of the compound layer

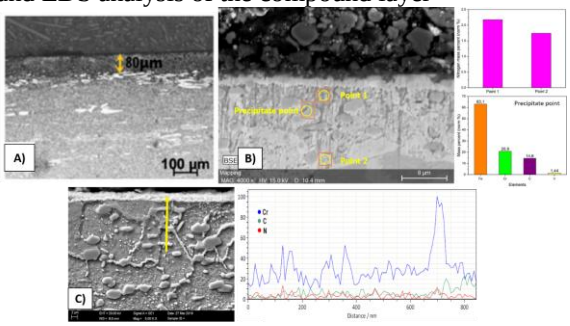

The EDS analysis performed by SEM shows the chemical composition of the precipitates, compound layer, and diffusion layer observed in the metallography of the treated material, which is presented in Figures 2 (b) and (c). In Figure 2(b), analyzing the precipitate, it was possible to observe the presence of iron, which appears in more quantity, approximately 63.1 wt.%, and chromium, carbon, and vanadium elements presenting in weight percentages of 20.9%, 14.6%, and 1.44%, respectively. This indicates that there was a possible formation of M_7C_3 chromium carbide, and the presence of vanadium is justified by the alloy elements from the material [19].

In Figure 2(c) we can observe the presence of elements Cr, C, and N, in which the nitrogen is from the nitriding treatment, while the chromium, in high quantities, as well as carbon, are found due to the alloy elements of the AISI D2 steel. Figure 2(b) also presents an EDS punctual analysis in the diffusion zone, indicating a decrease in nitrogen quantity in-depth in the layer.

Figure 3 presents the chemical analysis obtained by SEM/EDS evidencing the substrate precipitates. It is possible to observe the presence of carbon, chromium, iron, and vanadium, with a concentration of vanadium and chromium in the precipitate region.

Figure 3 – Chemical composition obtained by SEM/EDS on map a) metallography in the region of the chemical composition analysis and determination of b) total elements, c) carbon element, d) chromium element, d) iron elements, and e) vanadium element

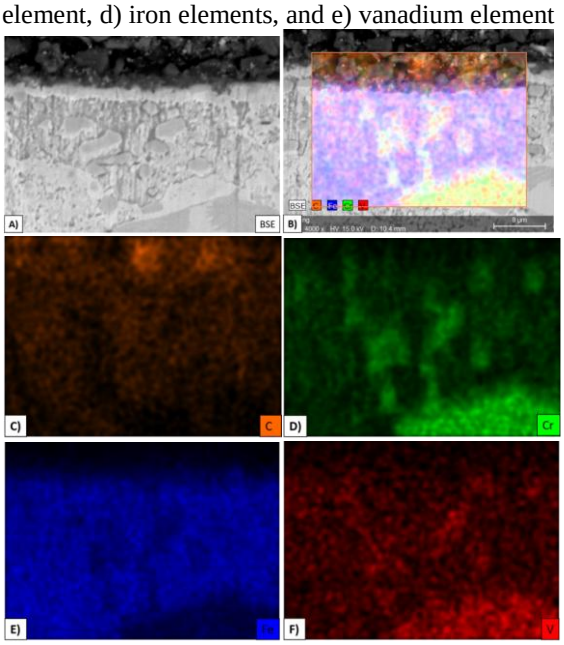

3.2 Microhardness test

Figure 4 presents the average hardness values found in each analyzed point, in that point 1 is positioned in the transition of the compound layer and diffusion zone, point 2 refers to the complex carbides zone, and point 3 is the substrate region. It is possible to observe that the hardness decreases in-depth with the nitrided layer due to nitrogen percentage reduction. The highest hardness was observed in point 1, with 550HV, proving the increase in the surface hardness of the material due to the plasma nitriding, which forms iron nitride as Fe_4N and $Fe_{2-3}N$, with presents ceramic characteristics and compressive tensions that increase the material hardness [20].

Figure 4 – Hardness Vickers a) point localization scheme and b) hardness values.

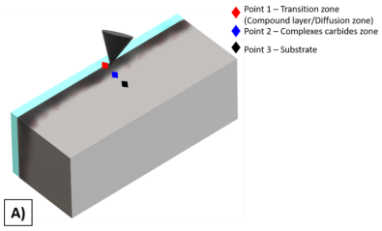

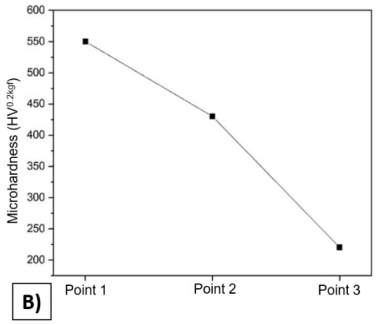

3.3 Micro-abrasive wear test

It is possible to observe in Figure 5 the wear volume as a function of sliding distance multiplied by the normal load applied in the test. The nitrided sample presented wear volume lower than the untreated material, which corroborates with microhardness results. However, as studied by Danelon et al. [8], a higher hardness does not always present a better wear resistance, because a hard layer can present fragile characteristics and easily detach from the substrate, impairing the nitriding treatment efficiency in wear resistance. The wear volume showed directly related to sliding distance, in that the increase in the sliding distance caused the increase in the wear volume, except for the 10 min test parameter to the treated material. For each test time and sliding distance the treated samples presented better wear resistance when compared to the base material, indicating the plasma nitriding effectiveness of the AISI D2 due to the improvement of the tribological properties of the studied material [10], [21].

Figure 5 – Wear volume (V) as a function of sliding distance multiplied by the normal load (SN)

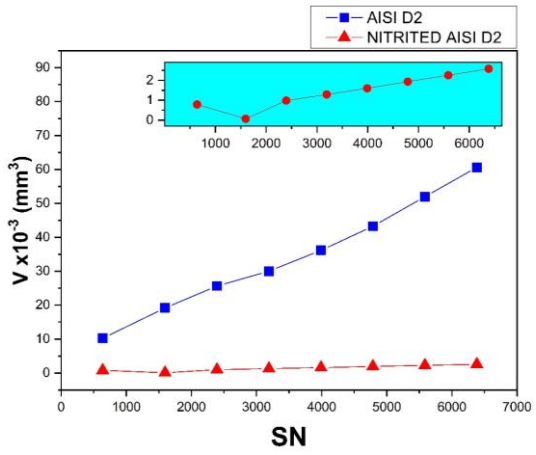

Figure 6 presents the crater obtained in the wear test, which is possible to observe a mix of the wear mode (grooving + rolling) in the base material, with a predominance of the grooving mode indicated by the vertical scars observed in the crater. According to

Mergler and Huis in 't Veld [22], the grooving mode occurs for a high load present in the region contact and low presence of abrasive liquid. In the nitrided sample, it is also possible to observe a mixed wear mode, but with a higher tendency to rolling wear mode, which occurs mostly when there is an abrasive liquid during the test. This occurs because the nitride layer produces debris during the wear test, and these particles act like an abrasive that rolls in the wear region [22], [23].

Figure 6 – Wear craters obtained at 450 seconds to a) untreated and b) treated material

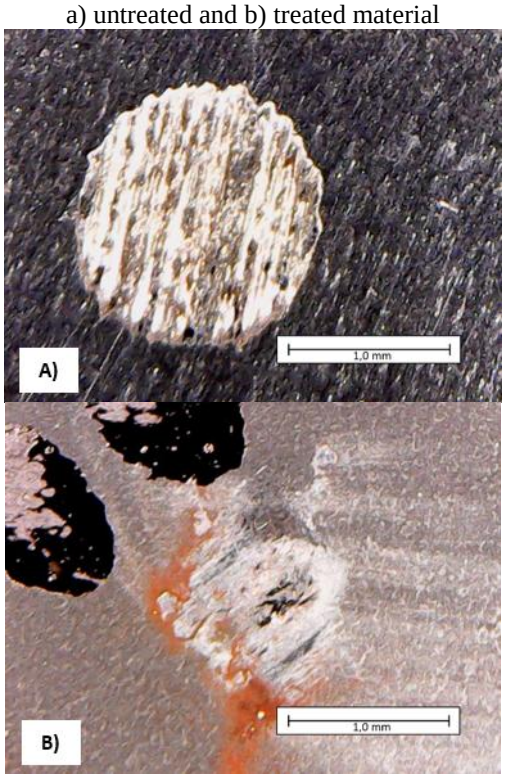

Figure 7 presents the wear volume as a function of sliding distance multiplied by the normal load applied in the test, presenting the linear regression equation related to the results. This graphic gives us information about the SSW. Generally, for micro-abrasive wear tests by fixed ball, the comparison between the wear resistance of two materials must be considered after the SSW achievement [13].

Figure 7 –Linear regressions obtained from the relation of the wear volume and SN parameters to determine the SSW regime.

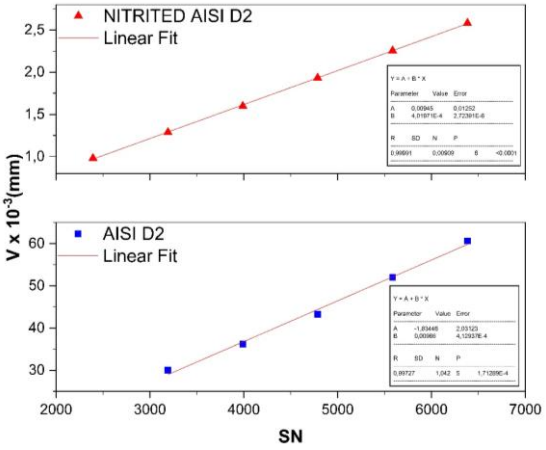

Thus, in Figure 8, it is also obtained the wear coefficient (k) through linear regression obtained from the experimental data of wear volume at the function of SN test parameters. The k parameter corresponds to the straight-line slope, identified as the "B" value in the graphic of Figure 8, whose parameter proves to be fundamental for this work analysis once its constancy along with the sliding distance represents the SSW [23].

Figure 8 – Friction coefficient of the base material and nitrided material

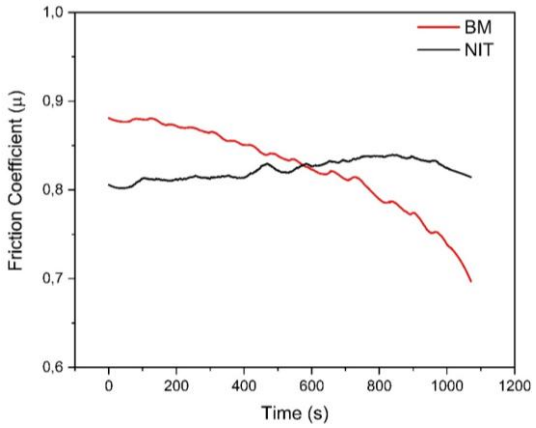

Nitrided AISI D2 steel presented wear coefficient of $k= 4.02x10^{-4} \pm 2.724x10^{-6} mm^3N^{-1}m^{-1}$ with R= 0.99991, significantly lower than the coefficient presented by the untreated AISI D2, whose value was $k = 9.66x10^{-3} \pm 4.129x10^{-4}$ $mm^3N^{-1}m^{-1}$ with R= 0.99727. This shows us the significant reduction of the wear severity occurred in the same test conditions due to the nitriding treatment. Such data may be indicating a high useful life of the nitriding material when applied in service, wherein a lower wear coefficient represents less severe wear.

Besides that, with the reach of the SSW, it is possible to predict the material wear behavior in

conditions that were not tested without the need for new tests. A mathematical development can be used to do it, through the replacement of the eq. 1 in the eq.2, obtaining the eq.3:

$$K = \frac{1}{SN} . V \qquad \text{(eq. 3)}$$

Isolating the wear volume (V) present in the eq.3, we can have:

$$V = KSN \qquad \text{(eq. 4)}$$

With the eq. 4, it is possible to determine the wear volume to longer distances, using the wear coefficient obtained experimentally as we can see in eq. 5 and 6. It is important to emphasize that the k value present in eq. 5 and eq.6 were obtained in the linear regression of the experimental data shown in Figure 8.

$$V = 4.02x10^{-4}SN \qquad \text{(eq. 5)}$$

$$V = 9.66x10^{-3}SN \qquad \text{(eq. 6)}$$

Using eq. 5 and 6, the wear volume to others testing times can be predicted. For example, the calculated wear volume for 1 hour of the test (3600 s) is 135,750.073mm^3 to the untreated tool steel AISI D2, while the wear volume of the nitrided AISI D2 is 5,774.071mm^3. The wear volume for the untreated AISI D2 steel was 95.85% higher than the nitrided material.

In eq. 5 and eq.6, the A value obtained in the linear regression presented in Figure 7 was not utilized because it is only possible to predict the wear behavior when the test reaches the SSW, and the A value represents the first points in the graphic where the line crosses the x-axis. In this position, the SSW is not reached, and the k parameter obtained by the mathematical development cannot be used.

However, the prediction of the useful life of a machine component in service is not easy once the friction and wear processes occur in dynamic and complex systems. Due to the strong inter-relations, irreversible and dissipative between the system components, the friction, and wear coefficient are features of the tribo-system and not intrinsic properties of the materials [24].

The representative friction coefficients of the treated and untreated material are presented in Figure 8. It is possible to observe that both samples presented friction coefficients in similar magnitudes but with different behaviors, once the friction coefficient decreases during the test time for the base material, while in the nitrided sample the friction coefficient increases during the test time. Thus, it is possible to affirm that parameters such as high hardness proportioned by the compound layer were more significant to improve the AISI D2 wear resistance than the friction coefficient [25].

According to Kusano and Hutchings [26], the rolling wear mode presents a lower magnitude of friction coefficient, and Cozza et al. [27] say that the grooving wear mode presents a higher magnitude of friction coefficient when compared to the rolling wear mode. Such results, presented in Figure 8 also corroborate with the wear mode identified in Figures 6 (a) and (b). The base material presented mixed wear mode and a friction coefficient drop throughout the test, which can be justified by the wear mode transition, from grooving to rolling mode, while the inverse occurred in the nitrided sample, in that the friction coefficient starts lower and increases its magnitude during the test time, which there is the transition from rolling to grooving.

IV. CONCLUSIONS

The obtained results in the present study evidenced the efficiency of the plasma nitriding treatment to increase the wear resistance of the studied material. Such results are justified by the formation of a compound layer on the surface of AISI D2 steel with presents a ceramic characteristic and high hardness providing a higher wear resistance when compared to the base material.

Another important point analyzed in this work was the obtention of the steady-state of wear, which promotes a higher tribological behavior precision of the studied material, wherein there is a wear volume linear behavior as a function of the sliding distance during the test. With this data, it was possible to determine a fixed wear coefficient for each analyzed sample.

The analysis of the friction coefficient shows us that the nitriding treatment, besides providing a significant reduction of the wear resistance when compared to the base material, provides a greater constancy of this parameter throughout the tests.

The improvement in the tribological properties of the treated material, originated by the nitriding treatment, can indicate a longer useful life to the tolls when applied to the material during service. This analysis can be performed using the wear coefficient as a function of the test sliding distance. The value of sliding distance can be converted to tool useful time from the fixed wear coefficient, and specific useful time can be found using linear regression in the SSW obtained from the experimental data if the wear test conditions are like wear service conditions. This obtained value can be associated with the nitride compound layer for the treated material, providing us the information on the useful life of the nitrided material predicting when

the compound layer might be consumed due to wear. This correlation can be done for similar wear parameters as used to obtain the SSW regime.

With this analysis, it is possible to determine that when compared to the base material, the nitrided AISI D2 steel would provide a longer useful life to the tool during service in the manufacturing industry sector, generating an increase in equipment maintenance or parts replacement.

REFERENCES

[1]. B. Ben Fathallah, C. Braham, H. Sidhom, Combined effects of abrasive type and cooling mode on fatigue resistance of AISI D2 ground surface, Int. J. Fatigue. 138 (2020). https://doi.org/10.1016/ j.ijfatigue.2020.105665.

[2]. E. da S. Costa, R.R.M. de Sousa, R.M. Monção, M.S. Libório, T.H. de C. Costa, Nitretação e deposição por plasma em ferramentas de aços AISI M2 e D2 utilizadas na conformação e estampagem de pregos: um estudo de viabilidade, Matéria (Rio Janeiro). 26 (2021). https://doi.org/10.1590/s1517-707620210001.1222.

[3]. H.S.M. Lopes, J.A. Moreto, M.D. Manfrinato, N.C. da Cruz, E.C. Rangel, L.S. Rossino, Micro Abrasive Wear Behaviour Study of Carburization and Ion Plasma Nitriding of P20 Steel, Mater. Res. 19 (2016) 686–694. https://doi.org/10.1590/1980-5373-MR-2015-0721.

[4]. J.O. Pereira Neto, R.O. da Silva, E.H. da Silva, J.A. Moreto, R.M. Bandeira, M.D. Manfrinato, L.S. Rossino, Wear and Corrosion Study of Plasma Nitriding F53 Super duplex Stainless Steel, Mater. Res. 19 (2016) 1241–1252. https://doi.org/10.1590/ 1980-5373-mr-2015-0656.

[5]. E. De Araújo, R.M. Bandeira, M.D. Manfrinato, J.A. Moreto, R. Borges, S.D.S. Vales, P.A. Suzuki, L.S. Rossino, Effect of ionic plasma nitriding process on the corrosion and micro-abrasive wear behavior of AISI 316L austenitic and AISI 470 super-ferritic stainless steels, J. Mater. Res. Technol. 8 (2019) 2180–2191. https://doi.org/10.1016/ j.jmrt.2019.02.006.

[6]. J.P.M. Shica, R.R.M. de Sousa, T.H. de C. Costa, R.M. Monção, P.L.C. Serra, M.G.C.B. Barbosa, F.R.C. De Macedo, L.H.P. De Abreu, prospecção tecnológica: deposição por plasma em gaiola catódica em pastilhas revestidas de metal duro / technological prospection: cathodic cage plasma deposition in hard metal discs, Brazilian J. Dev. 7 (2021) 19421–19427. https://doi.org/10.34117/ bjdv7n2-538.

[7]. F.A.P. Fernandes, S.C. Heck, C.A. Picone, L.C. Casteletti, On the wear and corrosion of plasma nitrided AISI H13, Surf. Coatings Technol. 381 (2020). https://doi.org/10.1016/j.surfcoat.2019.125216.

[8]. M.R. Danelon, F. Soares, M.D. Manfrinato, L.S. Rossino, Estudo do efeito da nitretação iônica a plasma na resistência ao desgaste do aço SAE 1020 utilizado em matriz de conformação, Rev. Bras. Apl. Vácuo. 39 (2020) 142. https://doi.org/10.17563/ rbav.v39i2.1166.

[9]. L. de A.P. de Campos, L.S. de Almeida, B.P. da Silva, M.R. Danelon, I.V. Aoki, M.D. Manfrinato, L.S. Rossino, Evaluation of Nitriding, Nitrocarburizing, Organosilicon Interlayer, Diamond-Like Carbon Film and Duplex Plasma Treatment in the Wear and Corrosion Resistance of AISI 4340 Steel, J. Mater. Eng. Perform. (2020). https://doi.org/10.1007/s11665-020-05277-9.

[10]. M.D. Conci, A.C. Bozzi, A.R. Franco, Effect of plasma nitriding potential on tribological behaviour of AISI D2 cold-worked tool steel, Wear. 317 (2014) 188–193.https://doi.org/10.1016/j.wear.2014.05.012.

[11]. R.C. Cozza, Influência do Desgaste da Esfera na Formação das Crateras de Desgaste em Ensaios Ball-cratering, Tecnol. Em Metal. Mater. e Mineração. 12 (2015) 202–210. https://doi.org/http://dx.doi.org/10.4322/2176-1523.0828.

[12]. W.C. Santos, J.O. Pereira Neto, R.O. da Silva, G. Rodriguês, J.A. Moreto, M.D. Manfrinato, L.S. Rossino, Desenvolvimento de dispositivo e estudo do comportamento ao microdesgaste abrasivo do aço AISI 420 temperado e revenido, Rev. Mater. 20 (2015). https://doi.org/10.1590/S1517-707620150002.0031.

[13]. R.C. Cozza, A.A.C. Recco, A.P. Tschiptschin, R.M. de Souza, D.K. Tanaka, Análise Comportamental dos Coeficientes de Atrito e Desgaste de Sistemas Revestidos Submetidos a Desgaste Micro-abrasivo, Tecnol. Em Metal. Mater. e Mineração. 6 (2010) 237–244. https://doi.org/10.4322/tmm.00604010.

[14]. K.L. Rutherford, I.M. Hutchings, A micro-abrasive wear test, with particular application to coated systems, Surf. Coatings Technol. 79 (1996) 231–239. https://doi.org/10.1016/0257-8972(95) 02461-

1.
[15]. R.C. Cozza, Estudo da obtenção do Regime Permanente de Desgaste em ensaios de desgaste micro-abrasivo por esfera rotativa conduzidos em corpos-de-prova de WC-Co P20 e aço-ferramenta M2, Matéria (Rio Janeiro). 23 (2018). https://doi.org/10.1590/s1517-707620170001.0322.
[16]. K.P. Lijesh, M.M. Khonsari, On the onset of steady state during transient adhesive wear, Tribol. Int. 130 (2019) 378–386. https://doi.org/10.1016/ j.triboint.2018.10.004.
[17]. D. da Cruz, B.A. de Souza, L. de A.P. de Campos, L.S. de Almeida, M.D.M. Jeferson Aparecido Moreto4, N.C. da Cruz, L.S. Rossino, Projeto , construção e comissionamento de um reator para tratamento de nitretação iônica a plasma em aço P20, Rev. Bras. Apl. Vac. 37 (2018) 102–113. https://doi.org/https://doi.org/10.17563/rbav.v37i3.1107.
[18]. L.S. de Almeida, A.R. Moreno de Souza, M.D. Manfrinato, L.S. Rossino, Estudo do efeito dos parâmetros do tratamento da limpeza a plasma na adesão e resistência ao desgaste de filmes DLC em liga de Ti6Al4V, Rev. Bras. Apl. Vácuo. 39 (2020) 42–55. https://doi.org/10.17563/rbav.v39i1.1161.
[19]. A.I. Gorunov, Investigation of M7C3, M23C6 and M3C carbides synthesized on austenitic stainless steel and carbon fibers using laser metal deposition, Surf. Coatings Technol. 401 (2020) 126294. https://doi.org/10.1016/j.surfcoat.2020.126294.
[20]. B.W. Hwang, C.M. Suh, H.K. Jang, Effects of Surface Hardening and Residual Stress on the Fatigue Characteristics of Nitrided SACM 645 Steel, Int. J. Mod. Phys. B. 17 (2003) 1633–1639. https://doi.org/10.1142/S0217979203019435.
[21]. L.A.S. Soares, L.S. de Almeida, R.R. Pavani, L.S. Rossino, M.D. Manfrinato, Influência da nitretação a plasma na resistência ao microdesgaste abrasivo e na corrosão ciclica do aisi 304, Boletim Técnico da Faculdade de Tecnologia de São Paulo,. 47 (2019) 18–24.
[22]. Y.J. Mergler, A.J. Huis in 't Veld, Micro-abrasive wear of semi-crystalline polymers, in: 2003: pp. 165–173. https://doi.org/10.1016/S0167-8922(03)80129-3.
[23]. R.C. COZZA, Estudo do comportamento do coeficiente de desgaste e dos modos de desgaste abrasivo em ensaios de desgaste micro-abrasivo, Escola Politécnica da Universidade de São Paulo, 2006.
[24]. H. Czichos, G. Salomon, The Application of Systems Thinking and Systems Analysis to Tribology, Der Bundesanstalt Für Mater. 30 (1974) 1–10.
[25]. S. Kumar, S.R. Maity, L. Patnaik, Friction and tribological behavior of bare nitrided, TiAlN and AlCrN coated MDC-K hot work tool steel, Ceram. Int. 46 (2020) 17280–17294. https://doi.org/10.1016/ j.ceramint.2020.04.015.
[26]. Y. Kusano, I.M. Hutchings, Sources of variability in the free-ball micro-scale abrasion test, Wear. 258 (2005) 313–317. https://doi.org/10.1016/ j.wear.2004.02.020.
[27]. R.C. Cozza, D.K. Tanaka, R.M. Souza, Friction coefficient and abrasive wear modes in ball-cratering tests conducted at constant normal force and constant pressure—Preliminary results, Wear. 267 (2009) 61–70. https://doi.org/10.1016/j.wear.2009.
[28]. 01.055.